

IDENTIFYING GENETIC FACTORS AFFECTING ANTHRACYCLINE-INDUCED CYTOTOXICITY

Brent D. Hehl

A thesis submitted to the faculty of the University of North Carolina at Chapel Hill in partial fulfillment of the requirements for the degree of Master of Science in the School of Medicine, Department of Pharmacology.

Chapel Hill
2012

Approved by:

Howard McLeod, PharmD

Robert A. Nicholas, Ph.D.

Alison Motsinger-Reif, Ph.D.

Terrence Kenakin, Ph.D.

©2012
Brent D. Hehl
ALL RIGHTS RESERVED

ABSTRACT

BRENT D. HEHL: Identifying Genetic Factors Affecting Anthracycline-Induced Cytotoxicity
(Under the direction of Howard McLeod, PharmD)

The molecular mechanisms responsible for anthracycline-induced cytotoxicity have been elusive despite intensive research over the past half century. Here, hits from a genome-wide association (GWA) screen seeking to identify genetic factors influencing drug-dose response were validated using a shRNA approach. The initial screen examined the phenotypic response of over 500 CHORI patient lymphoblastoid cell lines (LCLs) to the anthracyclines daunorubicin, epirubicin, and doxorubicin. Five candidate genes were identified from statistical correlation between intrinsic genomic differences and phenotype variability across the population of cell lines.

Of the 5 candidates selected (ADTRP, CSMD3, FHIT, PELI2, and SLC24A3), stable knockdown of PELI2 (and the positive control TOP2A) in LCLs were shown to have a significant effect on dose-dependent anthracycline response. While TOP2A has been previously established in the mechanism of anthracycline response, the identification of PELI2 in this screen is intriguing given recent work implicating NF- κ B signaling pathways in anthracycline response. These results establish shRNA-mediated gene-knockdown as a means to further validate GWA screens in LCLs.

To my parents

ACKNOWLEDGEMENTS

This body of work wouldn't exist without the contributions of a number of wonderful people, especially Tammy Havener, Bill Small, and Chad Brown. Thank you for providing generous amounts of your time, patience, and technical expertise.

For whom much is owed, Howard McLeod.
Your guidance will have a longstanding impact.

I'm very grateful to Carol Otey and Rob Nicholas
for their commitment and advocacy on my behalf.

The team at Gentriss, especially Scott Clark and Carrie Browning

Thank you to my fellow lab members, the Department of Pharmacology, and my committee
for the training and various engaging experiences along the way.

Many thanks go to those especially important people, my family and friends.
Without your support, such efforts wouldn't be worthwhile.

TABLE OF CONTENTS

LIST OF TABLES	vii
LIST OF FIGURES	viii
LIST OF ABBREVIATIONS	ix
CHAPTER 1: Background	1
CHAPTER 2: Materials and Methods	8
CHAPTER 3: Results	14
CHAPTER 4: Discussion	23
APPENDIX	27
REFERENCES	36

LIST OF TABLES

Table

1. Proportion of Raw Data Affected by Each Quality Control Step	11
2. Candidate Genes.....	16
3. Selected CHORI cell lines.....	17
4. Candidate Gene Knockdown p-values.....	20

LIST OF FIGURES

Figure

1. Cellular factors affecting doxorubicin (DOX) response.....	2
2. Anthracycline Chemical Structures.....	6
3. Doxorubicin GWAS.....	15
4. CHORI cell line selection.....	17
5. Generation of Stable Cell Lines.....	19
6. Effects of TOP2A and PELI2 reduction on drug dose-response.....	21

LIST OF ABBREVIATIONS

ADTRP: androgen-dependent TFPI-regulating protein

AUC: area under the curve

CHORI: Children's Hospital of Oakland Research Institute

CSMD3: CUB and Sushi multiple domains 3

CV: coefficient of variation

DMSO: dimethyl sulfoxide

DNA: deoxyribonucleic acid

DNR: daunorubicin

DOX: doxorubicin

EPI: epirubicin

FHIT: fragile histidine triad

GWA: genome-wide association

LCL: lymphoblastoid cell line

PELI2: pellino 2

PGx: pharmacogenomics or pharmacogenetics, interchangeably

RFU: relative fluorescence unit

shRNA: short hairpin RNA

SLC24A3: solute carrier family 24 (sodium/potassium/calcium exchanger), member 3

SNP: single nucleotide polymorphism

TOP2A: topoisomerase IIa

CHAPTER 1

BACKGROUND

While the promise of genetic screening and personalized medicine has yet to be fully realized in the post-Human Genome Project world [1], a better understanding of the influence of individual genetic variation on established methods of pharmacological intervention will positively affect current standards of care [2]. Tools that model genetic diversity, such as lymphoblastoid cell lines (LCLs), have proven effective in identifying loci affecting drug-response phenotypes [3]. This study employs the advantages (natural genomic variation and experimentally tractability) of the LCL system in efforts to better understand genes involved in the mechanism of anthracycline action.

Anthracyclines were first discovered in the early 1960s [4] and are among the most potent chemotherapeutics ever developed [5]. As a conventional cytotoxic cancer treatment, undesirable side effects are a key concern limiting their medical utility, with severe cardiotoxicity being recognized early in clinical development [6]. Tumor resistance [7] is also a clinical concern but the development and utilization of various combination drug therapy cocktails [5] have reduced its occurrence. By the early 1990s, an estimated 2000 analogues had been synthesized, with none more effective than the first anthracyclines, daunorubicin and doxorubicin [6]. The few derivatives in clinical use (epirubicin [8], idarubicin [9], and mitoxantrone [10]) may reduce toxicity and improve patient outcomes, but conflicting reports exist [11]. Balancing efforts to clarify the mechanism of action, reduce cardiotoxicity, and improve clinical effectiveness have long been a mainstay of anthracycline research [6].

Anthracycline antineoplastic, cardiotoxic, and drug resistance mechanism(s) are vigorously debated [11, 12]. Intriguingly, several different pathways are thought to mediate these effects (Figure 1), promising the hope of developing more effective and less toxic analogues. Anthracycline-DNA intercalation and damage induce cancer cell apoptosis, while in the heart, iron-mediated free radical generation has been shown to disrupt mitochondria to deleterious effect. Proposed resistance mechanisms include induction of drug metabolizing enzymes and transporters, as well as modulation of DNA damage and oxidative stress pathways [13].

Figure 1: Cellular factors affecting doxorubicin (DOX) response.

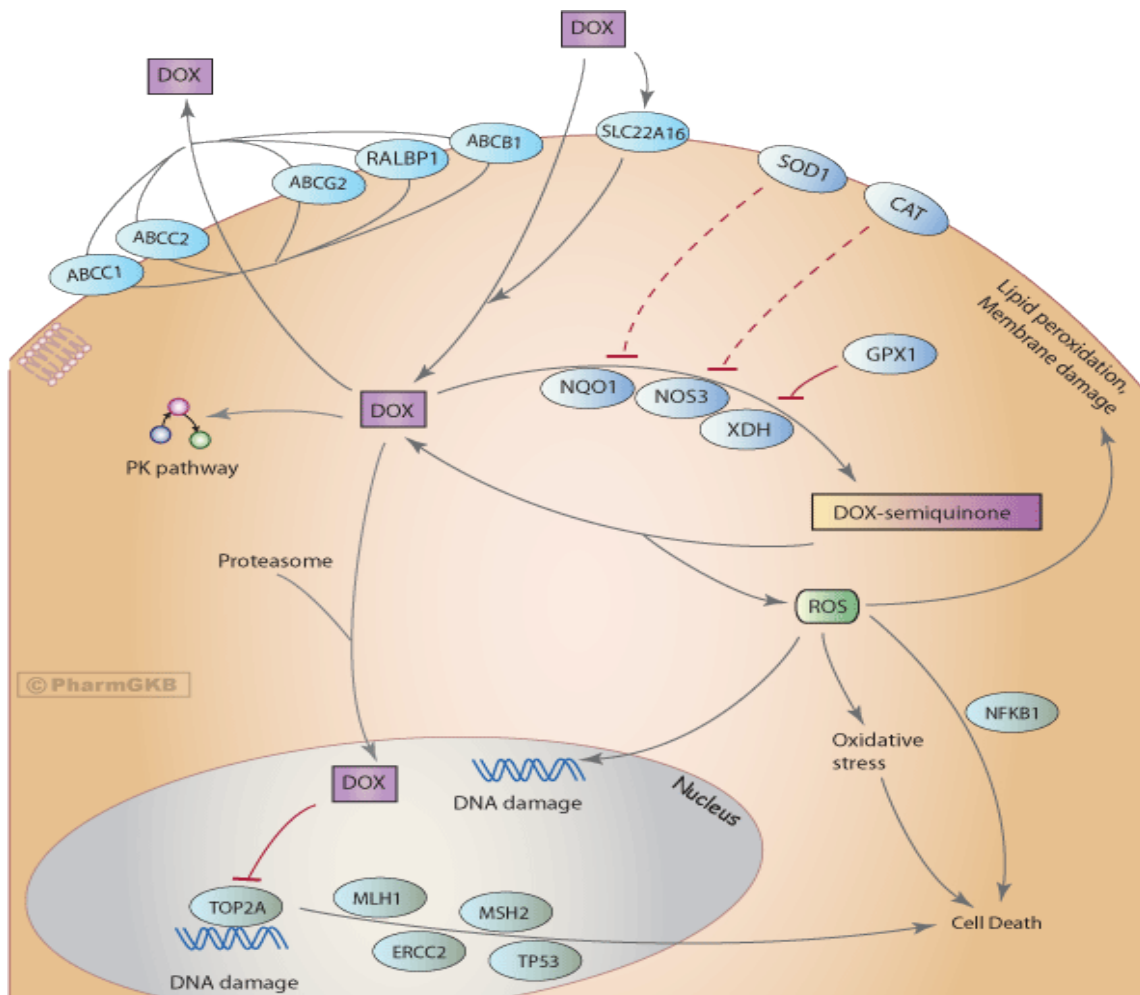


Figure 1: Continued

Rather than a single molecular target, a diverse set of cellular factors (transporters, oxidative signaling components, interactions with the proteasome, and DNA-repair/signaling proteins) contribute to doxorubicin's antineoplastic efficacy. It has been shown that tumors that establish chemo-resistance to DOX both modulate expression of and accumulate mutations within these pathways.

Antitumor activity: Early work in the 1970s revealed that anthracyclines bind nucleic acid and inhibit DNA synthesis [14], as well as induce protein-associated dsDNA breaks [15]. Topoisomerase II (TOP2A) [16, 17] was later discovered to mediate anthracycline-induced DNA lesions and activate DNA-damage apoptotic pathways, although the contribution of these pathways in the antitumor response isn't entirely clear in context of heterogeneous malignancies [18, 19]. Studies have also investigated the sequence specificity of anthracycline-DNA binding, which causes genotoxic stress by blocking transcription factor binding [20, 21]. Interestingly, anthracyclines also inhibit the proteasome, affecting protein turnover and cellular signaling [22]. Albeit controversial [12], the role of free radical formation also plays a role in apoptotic (nuclear signaling) and cardiotoxic (mitochondrial disruption) effects.

Cardiotoxicity: Two forms of cardiotoxicity manifest in response to anthracycline treatment. The relatively rare (1%) acute onset cardiotoxicity can be managed in the clinic and is mostly reversible, while the more serious chronic cardiotoxicity is a fairly grave prognosis. Intriguingly, these chronic side effects can also become manifest several years after the initial treatment. To date, restricting patients to a cumulative lifetime dose has been the most successful measure in mitigating cardiotoxicity [23]. The iron modulator dexrazoxane and methods to modulate anthracycline pharmacokinetics, such as liposomal formulations and slower infusions, have seen limited benefit [11] in mitigating this side effect.

Specific characteristics of cardiomyocytes related to oxidative capacity have been proposed to explain their susceptibility to anthracycline stress [24, 25]. In comparison to other tissues, the heart contains relatively low concentrations of regenerative antioxidants such as glutathione and catalase, and higher amounts of iron, an important metal species in the generation of reactive oxygen species. Anthracycline metabolites (oxidative stressors) have a long half-life and seem to preferentially accumulate in heart tissue [26]. As systemic blood levels of antioxidants also diminish upon anthracycline treatment, it is tempting to speculate that the heart may be exposed to a greater oxidative stress than it, as particularly susceptible to free radical damage, can reasonably accommodate. Many animal studies investigating the cardio-protective effects of various antioxidants in context of anthracycline treatment corroborate this line of reasoning, while similar protocols in human clinical trials have been disappointing in their inability to demonstrate any cardio-protective benefit [24].

Anthracycline Family

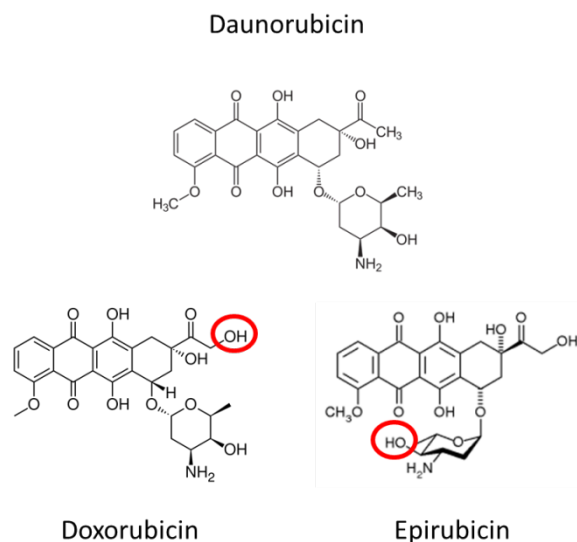
In the body of work described here, three members of the anthracycline family were examined: daunorubicin, doxorubicin, and epirubicin.

Daunorubicin [6]: Daunorubicin (DNR) was independently discovered by both Di Marco and Dubost in the late 1950s and early 1960s. A natural product from the soil microbe *Streptomyces peucetius*, it saw great use in the 70s and 80s against a wide variety of neoplasms. Other treatments have been developed against many of its original indications, but today it is still used upon occasion against acute myeloid and lymphocytic leukemias [27].

Doxorubicin [6]: Doxorubicin is very similar in chemical structure to DNR and can also be considered a natural product, however it was isolated from a mutagenized strain of *Streptomyces*. Approved after only six years of clinical testing, doxorubicin (DOX) is the most potent anthracycline and mainly used in highly effective liposomal preparations (Doxil™) against breast, small-cell lung, and ovarian carcinomas, and many sarcomas as well. Skin, colon and renal cancer are some of the few cancer types that do not respond to doxorubicin (DOX). Due to its incorporation into drug cocktails targeting a wide number of neoplasms, annual sales are currently maintained over \$500 million, nearly fifty years after its identification [28].

Epirubicin [6]: Epirubicin (EPI) was synthesized in the 1970s and shown to have similar efficacy as compared to DOX in animal models, but with a modified pharmacodynamic profile [29]. The small chemical difference from the parent daunorubicin molecule leads to faster elimination from the body, allowing EPI can be used at nearly twice the cumulative lifetime dose than DOX. While clinicians still adhere to a limited lifetime dosage to limit the risk of chronic cardiotoxicity, the increased clearance characteristics allow for more aggressive dosage regimens and improved response rates [30]. Myelosuppression becomes a concern under such conditions, but can be clinically managed more effectively than chronic cardiotoxicity. Epirubicin is mainly employed against breast, ovarian, stomach, and lung cancers, as well as certain lymphomas.

Figure 2: Anthracycline Chemical Structures



The three anthracyclines in our screen are remarkably similar, with the minor chemical differences from DNR highlighted in red.

Genome-Wide Association (GWA) studies

Genome-wide approaches [31-34] have been developed to interrogate drug function, examine biological mechanisms, and identify molecular targets. A more clear understanding of such information enables the development of next-generation pharmaceuticals that minimize underlying toxicity, resistance, and/or boost efficacy.

Lymphoblastoid cell lines (LCLs) approximately model healthy human cells [3] and offer certain advantages over comparative studies in yeast [31] and human cancer cell models [32]. >500 CHORI (Children's Hospital of Oakland Research Institute) LCLs [35] were previously both phenotyped for anthracycline (DNR, DOX, EPI) dose-response and profiled across the genome at single nucleotide polymorphism (SNP) resolution. Here, SNPs arising from the screen as effectors of drug response were identified and further refined into a candidate gene list for

further validation. A modified dose-response assay utilizing shRNA gene knockdown and anthracycline sensitive and resistant CHORI cell lines was developed and employed to determine if candidate gene knockdown would affect cell viability in response to anthracycline exposure and if so, if the effect was consistent across the entire drug class. Of the five candidate genes interrogated, the results of this study indicate knockdown of PELI2 sensitizes CHORI cells to all three anthracyclines in a consistent manner. This result is consistent with recent findings implicating NF- κ B signaling in anthracycline pharmacology.

CHAPTER 2

MATERIALS AND METHODS

Cell Culture

CHORI (Children's Hospital of Oakland Research Institute) generously donated EBV-transformed lymphoblastoid cell lines [35]. These CHORI lines were cultured in Roswell Park Memorial Institute (RPMI) medium (Invitrogen) supplemented with 15% fetal bovine serum (Sigma) and 100U/mL Penicillin and Streptomycin (Cellgro).

For stable cell line selection, Puromycin was added to the media at a final concentration of 1.0 $\mu\text{g/mL}$. Cell cultures were incubated at 37°C and 5% CO₂ in a humidified incubator. A Z1 Coulter Particle Counter (Beckman Coulter) was used to count cell concentrations. Cell lines were frozen into aliquots for use in future experiments and a new vial was used for each of the three replicates performed in this study.

Production of Lentiviral Particles

pLKO.1 shRNA bacterial stocks were obtained from OpenBiosystems and TRC1 shRNA libraries were constructed at the University of North Carolina-Chapel Hill Lenti-shRNA core facility. For each gene, 5 distinct shRNA plasmids were obtained, as detailed in Supplemental Table 1. Bacterial stocks were inoculated in Terrific Broth medium (MP Biomedicals) containing 100 $\mu\text{g/mL}$ of Carbenicillin (Invitrogen) and DNA isolated via MidiPrep kits (Qiagen).

For each transfected plasmid, 1×10^6 HEK-293T cells were seeded into a 6 cm cell culture dish overnight. The media was replaced with 5 mL antibiotic-free media for 8 hours. The transfection was then performed using 1 μ g of each pLKO.1 shRNA plasmid with 750 ng of psPAX2 packaging plasmid and 250 ng pMD2.G envelope plasmid in 20 μ l of serum-free OPTI-MEM (Invitrogen). The plasmid DNA mixture was mixed with 80 μ l of OPTI-MEM containing 6 μ l FuGENE 6 (Promega) and incubated for 30 minutes. The mixture was then added to the HEK-293T cells for 18 hrs, after which media was replaced with 5 mL fresh DMEM. The virus-containing media was collected and stored at 4°C 24h and 48h post-transfection, with 5 mL fresh media added to the cells after collection.

Transduction of Cell Lines

Five pools per each targeted gene of virus-containing media were combined and added to CHORI cell lines. One mL of transduction particle supernatant was added to 1 mL (1×10^6 cells) of each of the CHORI cell lines. Media was replaced after 24 hours and 1 μ g/mL of puromycin was added 48 hrs post-infection to select for transduced cells. Cells were under selection for 1 week with fresh puromycin added at day 4.

Knockdown Quantification

Western blots were performed using cell lysates to determine the extent of knockdown. Approximately 2×10^6 cells were lysed in RIPA buffer (Dulbecco's PBS, 0.1% Sodium Dodecyl Sulfate, 0.5% Sodium Deoxycholate, and 1% Igepal NP-40 supplemented with 1 mM PMSF, 1x complete protease inhibitor cocktail (Roche Diagnostics, Indianapolis, IN), and 1x Phosphatase

Inhibitor Cocktail 2 (Sigma, St. Louis, MO). An aliquot was used for protein quantitation determination using the BCA protein assay kit (Pierce Technology, Inc., St. Louis, MO). The remaining sample was mixed with 0.5 vol of 3x SDS sample buffer (1x equals 31.25 mM Tris-HCl (pH 6.8), 2% SDS, 5% 2-mercaptoethanol, 10% sucrose, and 0.005% bromophenol blue) and heated for 5 minutes at approximately 95°C. Equivalent protein amounts were run on SDS-PAGE in Tris/glycine/SDS buffer using 10% acrylamide gels. Resolved proteins were then transferred to PVDF membranes. The blots were blocked using a 5% solution of nonfat dry milk in 20mM Tris-HCl, pH7.4, 140mM NaCl, 0.1% Tween 20 and exposed to antibodies in the same buffer. Rabbit anti-human TOP2 (kind gift of Dr. Jack Griffith) was used to detect TOP2. Anti- β -actin (Sigma) was used as a loading control. Horseradish peroxidase-conjugated secondary antibodies were used as needed with ECL detection reagent (GE Healthcare Bio-Sciences Corp.) to visualize immunoreactive bands. Protein levels were quantified from autoradiographs scanned with an Agfa Duoscan T2500 scanner (Agfa Corp.) followed by densitometry using NIH Image 1.61.

Cytotoxicity assay

Cell lines infected with each lentiviral shRNA pool were plated at a density of 4,000 cells/well (45 μ L) in 384-well plates (Corning #3712) and treated with vehicle (water), doxorubicin, daunorubicin, or epirubicin (Sigma) over 12 concentrations (four replicates for each dose). Two cell lines were assayed per plate in the presence of 5 μ L of 10X [drug]. Seventy-two hours later, 5 μ L Alamar Blue (Invitrogen) was added to each well and fluorescence values (excitation: 535 nm, emission: 595nm) were acquired using the Tecan 1000 Multiplate Reader

(Tecan) 24 hours later. Three independent biological replicate experiments were performed, each with quadruplicate technical replicates for each experimental condition.

Quality control pipeline

The fluorescence data were processed through a quality control pipeline before being converted into percent cell viability at each drug concentration, per Equation 1 below. Briefly, any plate whose 90th percentile was below 2000 relative fluorescence units (RFUs) was assumed to contain mostly dead cells, and was removed from subsequent analysis. Next, positional effects (within a 2x12 group of 6 quadruplicate replicates, statistically significant ($p < 0.01$) with effect sizes > 1500 RFUs) were also examined. Third, a coefficient of variation (CV) screen was performed. If the CV > 0.2 , the deviate value was replaced with the mean of the other 3 non-deviant replicates. Finally, special care was taken with the 10% dimethyl sulfoxide (DMSO, negative) and vehicle (positive) controls, given their significant impact in calculating % viability. Mean viabilities from the 10% DMSO readings were checked to be within the biologically plausible range of 550 to 900 RFUs. The proportion of data affected by each step is given in Table 1.

Table 1: Proportion of Raw Data Affected by Each Quality Control Step

Step	Proportion
1	0.021
2	0.012
3	0.013
4	0.000

The high-throughput format of the experimental system is robust, as evidenced by less than 5% total of the overall data subject to quality control correction measures.

Percent viability was determined from each independent experiment per equation 1. Data were plotted and non-linear (Hill slope) curve fits were applied to generate dose-response graphs. These graphs were utilized to generate IC₅₀, Δ, and mean viability (AUC) values.

Equation 1:

$$\% Viability = \frac{\text{mean experimental RFU} - \text{mean negative control RFU}}{\text{mean vehicle RFU} - \text{mean negative control RFU}}$$

- Mean RFU (Relative Fluorescence Unit) values were derived from four wells.
- 10% DMSO serves as a negative control against background fluorescence due to media or cellular debris. Water served as vehicle for all drugs in this study.

Statistical analysis methodology

AUC responses were fit according to the linear mixed model in Equation 2, using SAS 9.2 with the procedure "proc mixed". The mixed models ANOVA is a generalization of the paired t-test that allows us to model across all the drug and target gene knockdown conditions together. This enables a better estimate of the effect contributed by of each component, more precise estimates for the variance of residuals, and ultimately, an increase in statistical power.

Equation 2:

$$AUC_{ijklm} = \mu + S_i + C_{ij} + G_k + D_l + R_m + GD_{kl} + SG_{jk} + CD_{ijl} + CDR_{ijlm} + \epsilon_{ijklm}$$

- AUC_{ijklm} is the AUC for the j^{th} cell line having sensitivity i , the k^{th} gene target, the l^{th} drug and the m^{th} replicate.
- Cell line is nested in sensitivity since each cell line has only one level of sensitivity, as opposed to the other factors, which are all crossed.
- To account for their correlation between observations, cell line and replication were modeled as random effects
- Sensitivity, Drug, and Gene effects were modeled as fixed effects.

CHAPTER 3

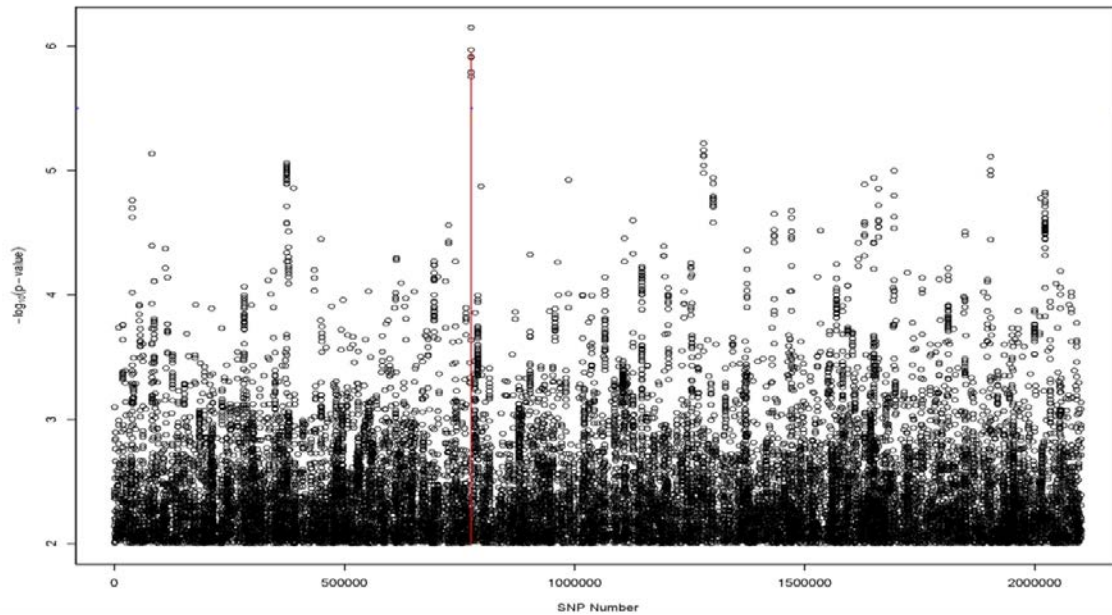
RESULTS

Genome-wide association analysis and candidate gene selection

Prior to the work performed here, drug-dose phenotypes were established for over 500 CHORI cell lines across the panel of 29 FDA-approved cytotoxic drugs as established in Peters et al. [36]. Genome-wide SNP profiles were also mapped for each cell line and nonparametric linkage analysis was utilized to identify genomic loci (“hits”) with putative correlation to variation in drug-dose response. Figure 3 outlines a visual representation (Manhattan plot) of the association data for doxorubicin.

With the large number of SNPs analyzed in a GWA study, hits are typically considered significant with p-values lower than 10^{-7} . As there were no results in this range for the initial screens of doxorubicin, epirubicin, and daunorubicin, a candidate list was built by identifying SNPs with the lowest p-values (ranging around 10^{-6}) that were common to at least two of the three drugs screened. The goal of this modified approach was to identify candidates that may affect the entire anthracycline drug class as opposed to a single member.

Figure 3: Doxorubicin GWAS



The relative genome coordinate of each scanned SNP is located on the x-axis (left to right: Chromosome 1 through Chromosome 23) with the negative log of the statistical association p-value on the y-axis. The greater the y-axis value, the stronger the association.

In order to evaluate the shRNA-mediated gene knockdown approach, the candidate SNP list was further refined to a list of candidate genes. None of the SNPs fell within the coding region of the genome, so the linkage disequilibrium (LD) of each SNP was examined through the the online SNAP (SNP Annotation and Proxy) tool available on the Broad Institute's website [37]. Based on this analysis, five candidate genes were selected (Table 2) for further validation. TOP2A was also included as a positive control for its relevance to the anthracycline drug-class and lentivirus containing an empty shRNA plasmid was used as a negative control. Finally, the phenotypic effect of each candidate gene knockdown was screened for each of the three anthracyclines.

Table 2: Candidate Genes

Gene	Official Name
TOP2A	topoisomerase IIa
PELI2	pellino 2
FHIT	fragile histidine triad
ADTRP	androgen-dependent TFPI-regulating protein
CSMD3	CUB and Sushi multiple domains 3
SLC24A3	solute carrier family 24 (Na/K/Ca exchanger), member 3

Selection of and generation of validation cell lines

Little to no information is available on the functional impact of each SNP on its respective candidate gene, so we sought to identify a subset of CHORI cell lines suitable for use in the candidate gene validation. As described in Brown et al. [38], various summary statistics are appropriate to describe drug dose-response. We utilized the average viability statistic (the cell line-specific viability average at each tested drug concentration, approximately proportional to area under the curve [AUC]) using the phenotype data from the original screen to identify the sensitivity of all CHORI cell lines to each of the anthracyclines doxorubicin, daunorubicin, and epirubicin. While IC_{50} is classically used to measure drug response, the viability statistic is also influenced by the shape of the hill slope curve and provides a more appropriate measure of response for our studies here. As seen in Figure 4, the cell lines displayed a robust correlation in dose-response across all three drugs. From the strength of these correlation data, the three most “sensitive” and “resistant” CHORI lines (Table 3) were selected and used for experiments with all three anthracycline drugs.

Table 3: Selected CHORI cell lines

Sensitive	Resistant
032098	032174
031634	040722
30349	021783

Figure 4: CHORI cell line selection

A) Each dot corresponds to an individual cell line in the original screen, with the same 5 **resistant** and **sensitive** lines depicted in each comparative plot. The cell lines were well correlated in response across all anthracyclines.

A) Averaged viabilities across all CHORI lines

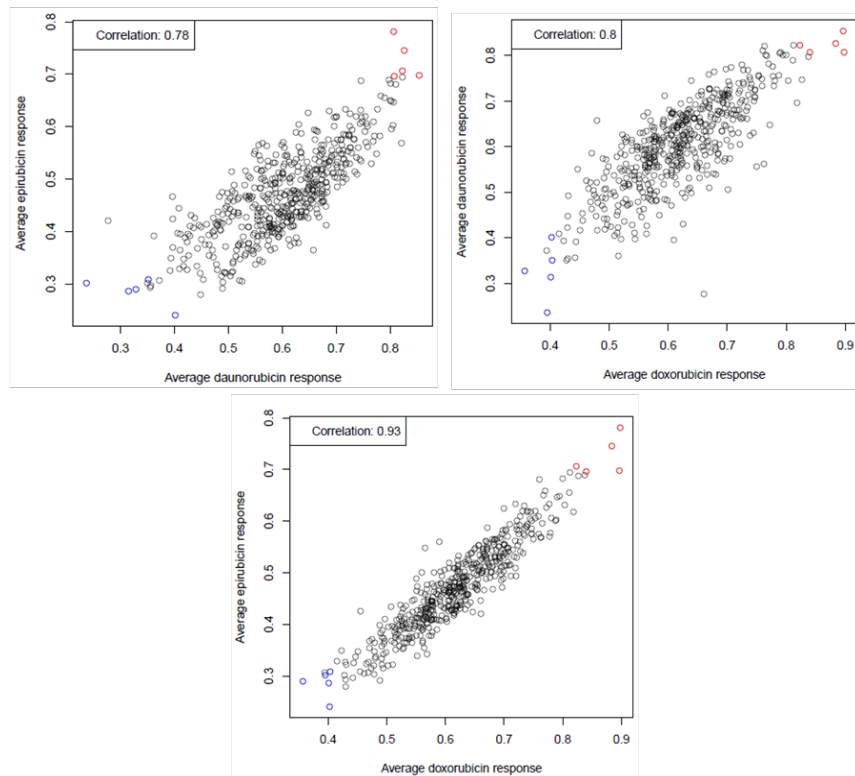
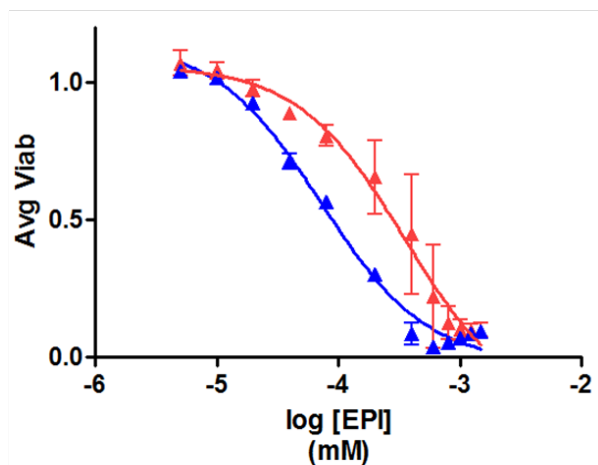


Figure 4: Continued

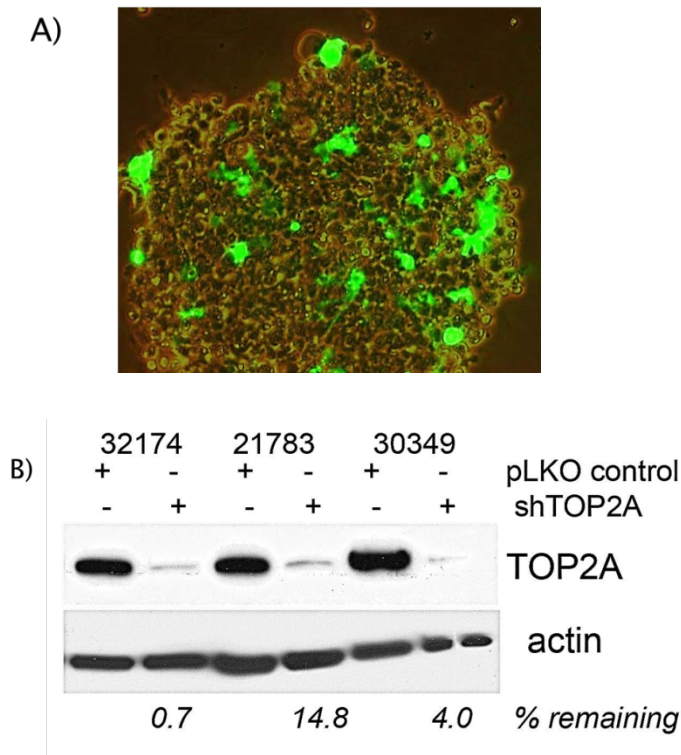
B) A dose-response plot of a representative sensitive and resistant cell line depicts the nearly 0.75 log difference in IC_{50} these lines have to epirubicin.

B) Dose-response curves of representative
'resistant' and 'sensitive' cell lines



As described in the Materials and Methods section, lentivirus pools were made (negative control = empty virus, positive control = shTOP2A, and 5 experimental shRNAs) and introduced to each of the 6 cell lines selected for validation. Of the 42 stable cell lines, three were unable to be established: 021784 shFHIT, 021784 shCSMD3, and 030349 shFHIT. After selection and establishment of the stable knock-down cell lines (Figure 5), dose-response experiments were performed as in the initial screen.

Figure 5: Generation of Stable Cell Lines



A) Infection of CHORI cells by lentivirus loaded with GFP expression plasmids indicates CHORI cells can be genetically manipulated, however at low efficiency. Puromycin selection was used to establish stable cell line populations.

B) Lysates from three cell lines (both shTOP2A and negative control) were probed for TOP2A protein expression three weeks after puromycin selection to demonstrate long-term, stable candidate gene knockdown.

Results of Candidate Gene Validation

Statistics (AUC, IC₅₀, and Hill-slope, see Supplemental Tables 1-3) were generated for each cell line and the AUC statistics were fit to a linear mixed model per Equation 2 (Materials and Methods), from which two hypotheses were tested:

Hypothesis 1: Does gene knockdown affect viability in response to anthracycline exposure?

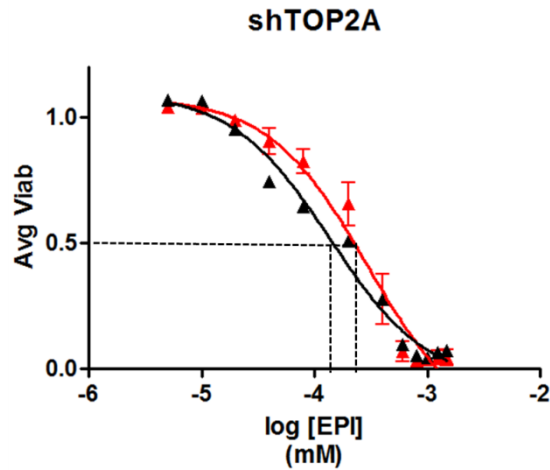
In this model, a significant percentage of the AUC variability was explained by the gene target (Table 4). After controlling for the effects of replicate, cell line, and drug treatment, PELI2 ($p < 0.0014$) and TOP2A ($p < 0.0006$) (Figure 6) were significantly different in comparison to controls, with PELI2 knockdown conferring a sensitizing effect and TOP2A a resistance effect. Although not quite meeting the threshold of resistance, FHIT ($p = 0.0522$) also had a sensitizing response. Of the six cell lines screened in our validation study, generation of stable FHIT knockdown in 030349 (sensitive) and 021783 (resistant) cell lines was unsuccessful and may influence the FHIT result.

Table 4: Candidate Gene Knockdown p-values

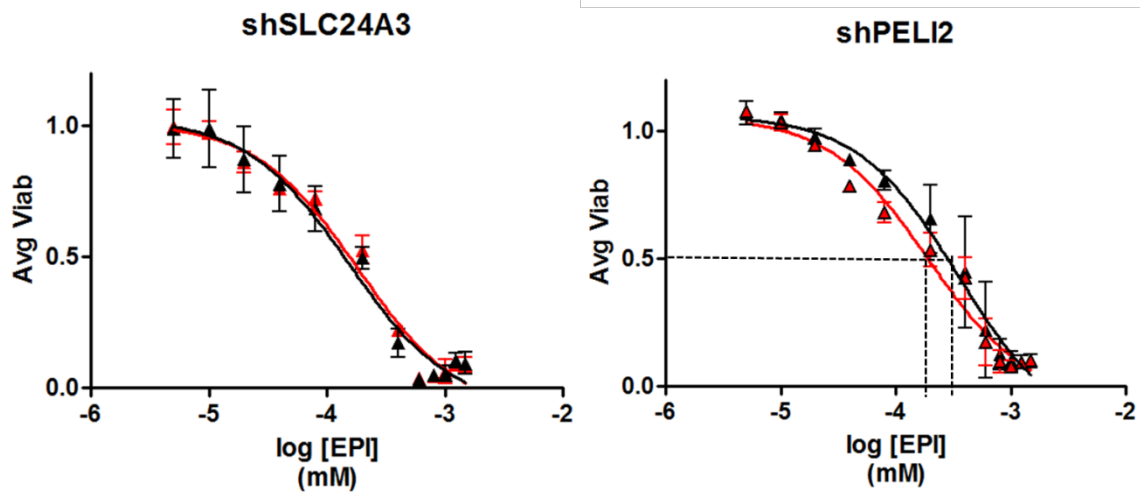
shRNA	P-value
ADTRP	0.0968
CSMD3	0.701
FHIT	0.0522
PELI2	0.0014
SLC24A3	0.2624
TOP2A	0.0006

The positive control TOP2A and candidate PELI2 were both shown to significantly affect anthracycline drug-dose response, with reduction of PELI2 sensitizing cells, and TOP2A knockdown causing resistance.

Figure 6: Effects of TOP2A and PELI2 reduction on drug dose-response



TOP2A reduction served as a positive control in this study and authenticated the validation assay's ability to identify genetic loci important to anthracycline response. shTOP2A cell lines (red) were approximately 1.75 fold more resistant (via IC₅₀) to epirubicin than negative controls (black), a consistent effect across the drug class.



ADTRP, CSMD3, FHIT, and SLC24A3 failed to validate in this study. A representative dose-response plot is shown for SLC24A3. In contrast, reduction of PELI2 sensitizes CHORI cells approximately 2X.

Hypothesis 2: Are viability effects consistent for the entire drug class versus a specific drug?

The model tested if the interaction between drug and gene target is significant. A significant result would indicate that at least one drug responds significantly differently than the other two for at least one gene target. The p-value for this result is not significant at 0.9809, signifying all gene knockdown associated variation seen was consistent across all three anthracyclines.

CHAPTER 4

DISCUSSION

The primary goal of these experiments was to validate hits arising from a pharmacogenomics screen employed to identify variant loci that affect anthracycline dose response. As an important piece of this screening approach, these data are expected to yield new insight into biological mechanisms of anthracycline efficacy and/or identify potential genomic indicators of response and toxicity. The findings indicate that 1) dose-response assays utilizing lentivirus to mediate shRNA gene knockdown are an effective validation strategy; 2) of the candidate genes tested, PELI2 (described further below) is the strongest candidate for further studies investigating its role in anthracycline response; and 3) average viability and AUC are valid statistics to measure drug response.

Method Validation

While LCL-based, drug-dose phenotype assays are a useful tool for enabling clinically-relevant SNP discovery, follow-up studies in relevant tissues and clinical cohorts are needed to validate their findings [3]. We've determined here that a) Epstein-Barr Virus-transformed LCLs can be transfected via shRNA-containing lentivirus to generate stable gene knock-down; and b) significant change in drug-dose response can be detected in these cell lines. Utilizing this method as an intermediary validation step before continuing to clinical cohorts will prove useful.

Topoisomerase IIa is a well-established molecular target for anthracyclines [16, 17] and as such, TOP2A-deficient LCLs were generated and tested to determine if the dose-response assay could detect a phenotypic response. As shown by statistically significant increase in AUC ($p < 0.0006$, Supplemental Table 6), cells with reduction in TOP2A were more resistant to anthracyclines. Interestingly, it has also been shown that drug-resistant tumors have similar changes in TOP2A protein levels [18].

Candidate Gene Validation

Of the five candidate genes examined, reduction of ADTRP, CSMD3, and SLC24A3 failed to show any significant cellular response to DNR, DOX, or EPI. While little is known of their individual endogenous functions, it is interesting to consider CSMD3 was recently shown in a whole-exome sequencing analysis to be the second-most mutated gene in lung cancer behind TP53 [39]. Our results do not conclusively exempt the possible impact of these genes on cancer biology, but rather leave them open to future examination. In conjunction with previous evidence, our data support a further investigation of the hits validated in this study.

PELI2: Studies have identified pellino 2, or PELI2, as an important signaling scaffold involved in IL-1-mediated activation of NF- κ B [40]. PELI2 modulates NF- κ B dynamics through its RING E3-ubiquitin-ligase activity [41] and has also been shown to activate MAPK pathways [42]. A significant node in acquired chemotherapy-resistance [43, 44], NF- κ B signaling mediates resistance to anthracyclines [45, 46] and has also been implicated in cardiotoxicity [47].

Our studies show knock-down of PELI2 confers anthracycline sensitivity ($p < 0.0014$) and highlights the significance of NF- κ B signaling in chemoresistance. It should be noted that after development, PELI2 expression is restricted primarily to tissues involved in the innate immune

response [40] and may explain its demonstrable effect in our particular cell system. Further studies examining PELI2 involvement in cancer-specific NF- κ B activation may prove clinically relevant given many cancers are thought to undergo “dedifferentiation” [48]. The role of NF- κ B inhibition in reducing both anthracycline-induced cardiotoxicity [47] and drug-resistance [44] lends considerable weight to further exploration of this pathway and its many regulatory modulators.

FHIT: FHIT reduction was seen to sensitize cells to anthracycline exposure, though our results were not statistically significant ($p < 0.522$) and underpowered ($n=4$) when compared to the other candidate genes ($n=6$). Regardless, it is interesting to note that FHIT is thought to be a tumor-suppressor and loss or aberrant expression is a hallmark of many cancers of the breast and lung [49]. Further studies with larger samples sizes will be important in determining if our tentative result is biologically relevant.

Measuring drug ‘response’

As the study of pharmacogenomics has broadened awareness of the impact of genetic variability, additional methods to describe and analyze drug response are needed. Traditional summary measures, such as IC_{50} and hill slope, while convenient and straightforward, limit the assessment of all factors contributing to variability. While methods continue to improve [38], the descriptions of and conclusions from complex datasets generated from these experimental approaches need to be carefully evaluated and results validated in other systems.

Conclusions

While investigated extensively for over fifty years, a detailed understanding of the mechanisms of anthracycline antineoplastic function and cardiotoxicity remain elusive. Studies such as these exploit individual biological variation in efforts to identify novel genetic effectors. While our results implicate PELI2, the direct translational relevance of this finding is unclear. Further validation work will entail analysis in relevant cell and cancer model systems. Additional studies may also include direct genomic examination of patient cohorts, as a similar approach undertaken with the TOP1 inhibitor, temozolomide, confirmed a direct clinical correlate [50]. These steps to more fully understand how such variation affects human health will lead us closer toward the ambitious goal of “personalized medicine”.

APPENDIX

Supplemental Table 1:

AUC statistic, mean and standard deviation

Table A: Daunorubicin							
	Control	TOP2A	PELI2	FHIT	ADTRP	CSMD3	SLC24A3
32098	10.9 ± 0.51	10.7 ± 0.39	10.6 ± 0.36	10.6 ± 0.44	10.9 ± 0.87	10.7 ± 0.47	10.7 ± 0.33
32174	11.5 ± 0.45	11.4 ± 0.098	11.2 ± 0.27	11.5 ± 0.31	11.6 ± 0.43	11.6 ± 0.5	11.5 ± 0.27
40722	11 ± 0.42	11.1 ± 0.42	11.3 ± 0.23	10.6 ± 0.078	11.4 ± 1.3	10.5 ± 0.32	10.7 ± 0.42
31634	10.9 ± 0.46	11.6 ± 0.23	11.2 ± 0.042	11.1 ± 0.068	11.1 ± 0.14	11.6 ± 0.21	11.1 ± 0.3
30349	10.7 ± 0.27	10.8 ± 0.57	10.2 ± 0.37		10.5 ± 0.86	10.6 ± 0.17	10.6 ± 0.48
21783	11.5 ± 0.42	11.8 ± 1.4	11.3 ± 0.81		11.6 ± 0.71		11.8 ± 0.61
Table B: Doxorubicin							
	Control	TOP2A	PELI2	FHIT	ADTRP	CSMD3	SLC24A3
32098	8.57 ± 0.81	8.7 ± 0.55	7.97 ± 0.77	8.14 ± 0.75	8.44 ± 0.92	8.38 ± 0.52	8.49 ± 0.81
32174	10.2 ± 0.76	10.4 ± 0.26	9.39 ± 0.58	10.2 ± 0.7	10.4 ± 0.87	10.4 ± 0.32	10.1 ± 0.67
40722	9.07 ± 0.37	8.78 ± 0.44	8.44 ± 0.19	8.21 ± 0.75	9.54 ± 1.3	8.13 ± 0.34	8.83 ± 0.38
31634	9.03 ± 0.63	10 ± 0.35	9.23 ± 0.52	9.18 ± 0.7	9.3 ± 0.64	9.87 ± 0.31	9.39 ± 0.7
30349	8.4 ± 0.65	8.78 ± 1.1	7.71 ± 1		8.56 ± 1.5	8.4 ± 0.64	8.58 ± 1.2
21783	10.4 ± 1	10.5 ± 1.8	9.88 ± 1.6		10.2 ± 1.8		10.6 ± 1.3
Table C: Epirubicin							
	Control	TOP2A	PELI2	FHIT	ADTRP	CSMD3	SLC24A3
32098	5.17 ± 0.54	5.13 ± 0.39	4.84 ± 0.42	4.79 ± 0.55	4.93 ± 0.55	4.98 ± 0.19	5.13 ± 0.49
32174	6.67 ± 0.51	6.99 ± 0.25	5.99 ± 0.59	6.51 ± 0.79	6.77 ± 0.97	6.59 ± 0.54	6.58 ± 0.65
40722	5.33 ± 0.56	5.35 ± 0.23	4.95 ± 0.32	4.99 ± 0.52	5.79 ± 1	4.98 ± 0.25	5.38 ± 0.11
31634	5.26 ± 0.36	5.93 ± 0.38	5.43 ± 0.4	5.31 ± 0.52	5.45 ± 0.48	5.95 ± 0.2	5.54 ± 0.42
30349	4.62 ± 0.97	5.18 ± 0.7	4.63 ± 0.62		5.12 ± 0.96	4.98 ± 0.35	5.08 ± 0.74
21783	7.18 ± 1.7	7.47 ± 2.1	6.7 ± 2.1		6.8 ± 2.2		7.4 ± 2.1

Supplemental Table 2:

log IC₅₀ statistic, mean and standard deviation

Table A: Daunorubicin							
	Control	TOP2A	PELI2	FHIT	ADTRP	CSMD3	SLC24A3
32098	-9.86 ± 0.095	-9.86 ± 0.12	-9.89 ± 0.047	-9.89 ± 0.1	-9.97 ± 0.1	-9.82 ± 0.17	-9.93 ± 0.049
32174	-9.49 ± 0.62	-10 ± 0.055	-9.06 ± 1.2	-9.56 ± 0.57	-9.97 ± 0.18	-9.81 ± 0.22	-9.82 ± 0.037
40722	-9.38 ± 0.84	-10 ± 0.2	-10.1 ± 0.12	-9.72 ± 0.37	-10 ± 0.15	-9.74 ± 0.28	-10 ± 0.051
31634	-9.84 ± 0.099	-10 ± 0.25	-10.1 ± 0.18	-9.78 ± 0.14	-10.2 ± 0.21	-9.95 ± 0.22	-9.85 ± 0.51
30349	-9.91 ± 0.093	-9.91 ± 0.12	-9.98 ± 0.11		-10 ± 0.086	-10 ± 0.13	-9.88 ± 0.052
21783	-9.83 ± 0.1	-9.81 ± 0.19	-11.2 ± 2.3		-13 ± 4.8		-8.88 ± 1.8
Table B: Doxorubicin							
	Control	TOP2A	PELI2	FHIT	ADTRP	CSMD3	SLC24A3
32098	-9.05 ± 0.48	-9.01 ± 0.18	-9.39 ± 0.34	-9.21 ± 0.31	-9.28 ± 0.32	-9.19 ± 0.16	-8.95 ± 0.49
32174	-8.61 ± 0.67	-7.84 ± 0.18	-9.35 ± 0.54	-7.6 ± 0.85	-9.01 ± 0.89	-8.48 ± 0.49	-8.41 ± 0.35
40722	-8.65 ± 0.095	-8.66 ± 0.17	-9.27 ± 0.28	-9.22 ± 0.57	-8.72 ± 0.33	-9.26 ± 0.015	-8.55 ± 0.081
31634	-8.61 ± 0.29	-8.17 ± 0.38	-8.51 ± 0.53	-8.54 ± 0.46	-8.51 ± 0.56	-8.24 ± 0.34	-8.33 ± 0.57
30349	-9.14 ± 0.56	-9.14 ± 0.73	-9.64 ± 0.68		-8.99 ± 0.83	-9.54 ± 0.29	-9.03 ± 0.77
21783	-8.04 ± 0.31	-8.7 ± 0.38	-9.38 ± 1.2		-10.7 ± 2.8		-8.67 ± 1.1
Table C: Epirubicin							
	Control	TOP2A	PELI2	FHIT	ADTRP	CSMD3	SLC24A3
32098	-9.42 ± 0.56	-9.29 ± 0.12	-9.53 ± 0.37	-9.55 ± 0.38	-9.6 ± 0.4	-9.36 ± 0.13	-9.39 ± 0.4
32174	-8.25 ± 0.64	-7.76 ± 0.14	-8.73 ± 0.82	-8.16 ± 0.54	-7.95 ± 0.55	-8.18 ± 0.5	-8.22 ± 0.5
40722	-8.71 ± 0.38	-8.81 ± 0.18	-9.8 ± 0.51	-9.44 ± 0.27	-8.67 ± 0.31	-9.58 ± 0.092	-8.67 ± 0.11
31634	-8.85 ± 0.2	-8.31 ± 0.19	-8.72 ± 0.54	-8.86 ± 0.39	-8.6 ± 0.46	-8.26 ± 0.18	-8.59 ± 0.3
30349	-9.19 ± 0.37	-9.33 ± 0.65	-9.87 ± 0.61		-9.18 ± 0.76	-9.72 ± 0.37	-9.46 ± 0.66
21783	-8.24 ± 0.73	-8.46 ± 0.95	-8.55 ± 1.1		-8.3 ± 1.1		-8.22 ± 0.78

Supplemental Table 3:

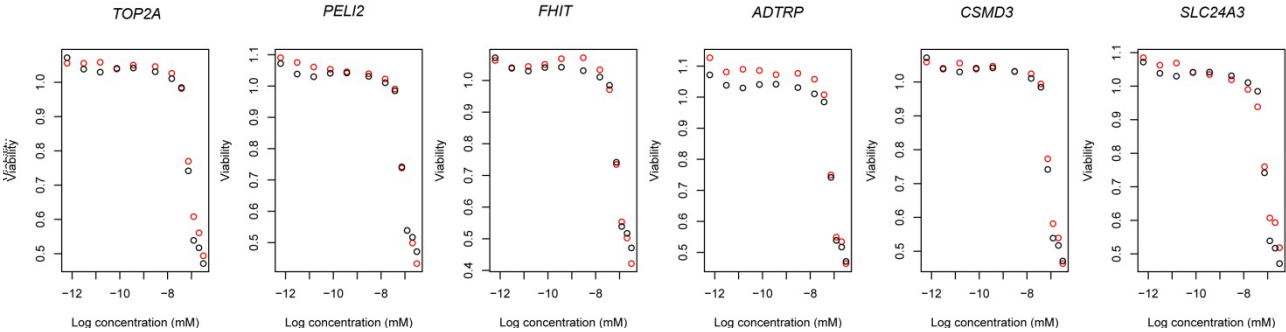
Hill-slope statistic, mean and standard deviation

Table A: Daunorubicin							
	Control	TOP2A	PELI2	FHIT	ADTRP	CSMD3	SLC24A3
32098	-30 ± 8.2	-26.5 ± 4.9	-29.9 ± 8.8	-26.8 ± 3.7	-30.4 ± 0.86	-30.5 ± 6.7	-20.2 ± 2.1
32174	-26.6 ± 19	-25.6 ± 1.9	-12.6 ± 5.3	-16.4 ± 8.1	-32.5 ± 14	-24.7 ± 8.9	-22.7 ± 4.7
40722	-15 ± 8.4	-26.5 ± 7.3	-24.5 ± 12	-17.7 ± 2.2	-27.1 ± 18	-15.1 ± 5.6	-29.8 ± 9.7
31634	-29 ± 3.4	-27 ± 10	-34.2 ± 1.1	-19 ± 5.2	-23.7 ± 9.1	-28.5 ± 3.4	-17.7 ± 3.7
30349	-25.7 ± 6.7	-28.5 ± 4.8	-26.7 ± 8.9		-34.8 ± 10	-30.1 ± 2.4	-28.3 ± 9
21783	-18.6 ± 6.6	-16.6 ± 5.9	-9.99 ± 7.9		-8.37 ± 3		-15.8 ± 13
Table B: Doxorubicin							
	Control	TOP2A	PELI2	FHIT	ADTRP	CSMD3	SLC24A3
32098	-10.8 ± 2.1	-11.7 ± 1.9	-11.7 ± 0.84	-10.6 ± 1.8	-10.8 ± 1.8	-11.3 ± 1.2	-9.65 ± 0.73
32174	-8.56 ± 2.6	-6.27 ± 1.4	-7.54 ± 0.94	-5.73 ± 2.5	-7.97 ± 1.5	-7.67 ± 1.6	-9.56 ± 3.2
40722	-9.64 ± 1	-10.5 ± 0.45	-9.66 ± 1.5	-10.5 ± 1.2	-9.28 ± 1.4	-8.82 ± 0.97	-10.5 ± 1.2
31634	-10.4 ± 2	-10.7 ± 2.9	-8.72 ± 2.1	-9.48 ± 1.9	-9.18 ± 1.3	-9.1 ± 1.3	-8.25 ± 1.6
30349	-10.2 ± 2.9	-13 ± 2.3	-14.4 ± 6.6		-9.74 ± 2.2	-11.3 ± 2.1	-11.6 ± 2.8
21783	-7.31 ± 1.5	-11.2 ± 3.6	-8.36 ± 0.9		-6.16 ± 2.9		-6.46 ± 3.6
Table C: Epirubicin							
	Control	TOP2A	PELI2	FHIT	ADTRP	CSMD3	SLC24A3
32098	-12.8 ± 2	-12.9 ± 0.56	-13.3 ± 1.1	-11.6 ± 1	-11.3 ± 1.6	-11.5 ± 2.1	-13.1 ± 0.19
32174	-13.1 ± 3.4	-15.7 ± 11	-7.63 ± 0.96	-16.2 ± 4.7	-16.6 ± 6.4	-18.2 ± 12	-19 ± 9.6
40722	-17 ± 6.3	-12.7 ± 1.8	-10.7 ± 2.2	-11.8 ± 0.29	-12.4 ± 2.5	-9.92 ± 0.83	-12.1 ± 2.2
31634	-10.9 ± 0.44	-17 ± 3.2	-10.2 ± 2.8	-11 ± 1	-14.6 ± 6.9	-16.4 ± 4.7	-13.5 ± 6.4
30349	-17.1 ± 7.7	-13.7 ± 0.98	-12.6 ± 2.2		-11 ± 2	-11.3 ± 1.5	-13 ± 0.85
21783	-22 ± 15	-19.7 ± 13	-18.1 ± 8.7		-23.4 ± 16		-23.6 ± 9.1

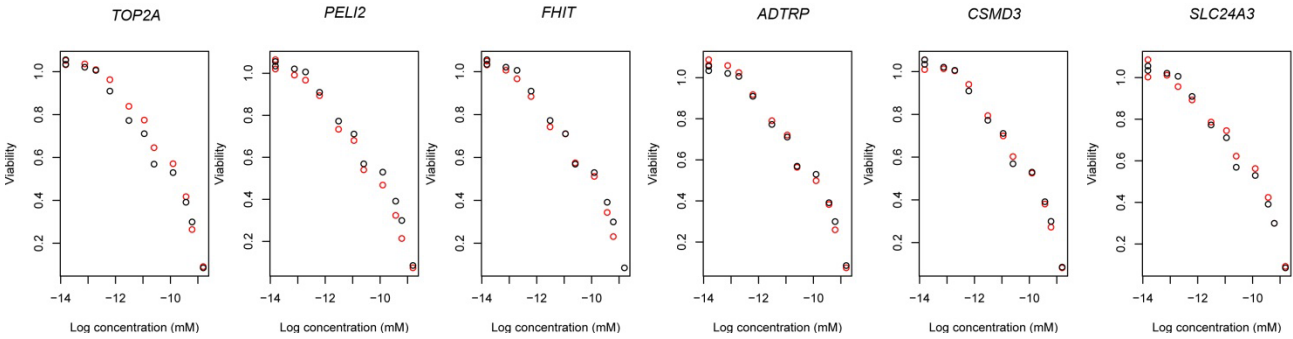
Supplemental Figure 1a:

CHORI line 032098

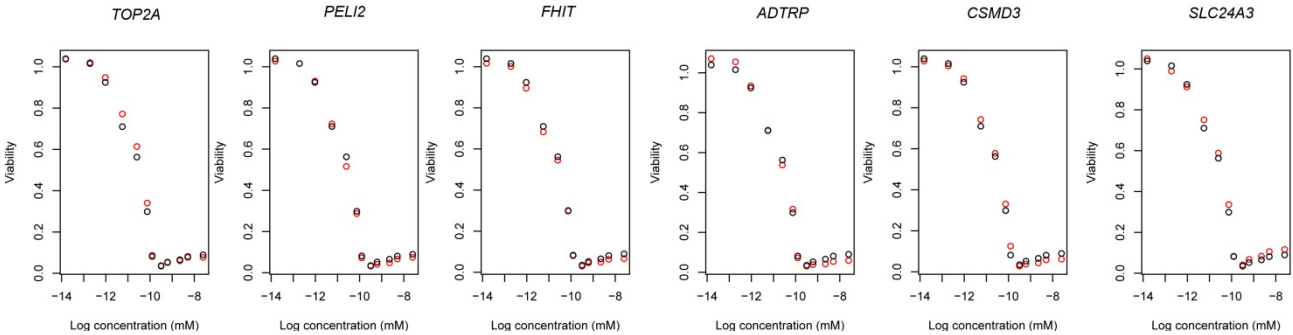
Daunorubicin response



Doxorubicin response



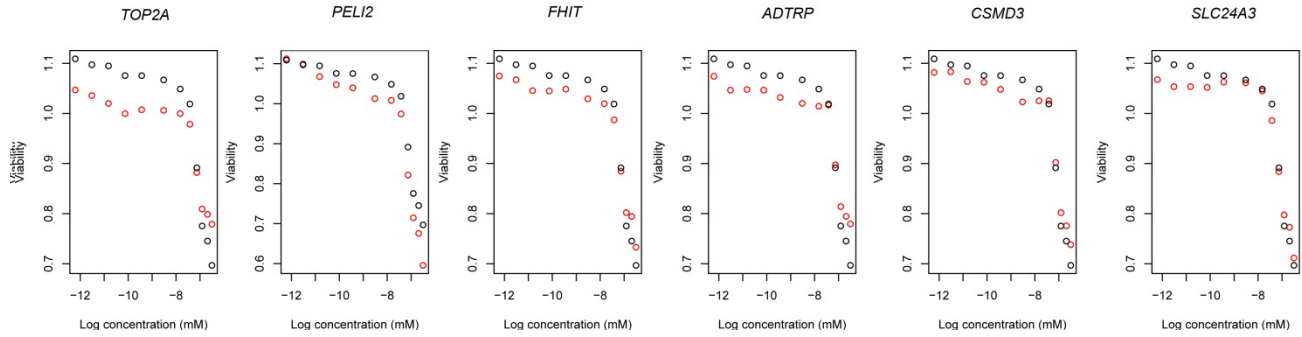
Epirubicin response



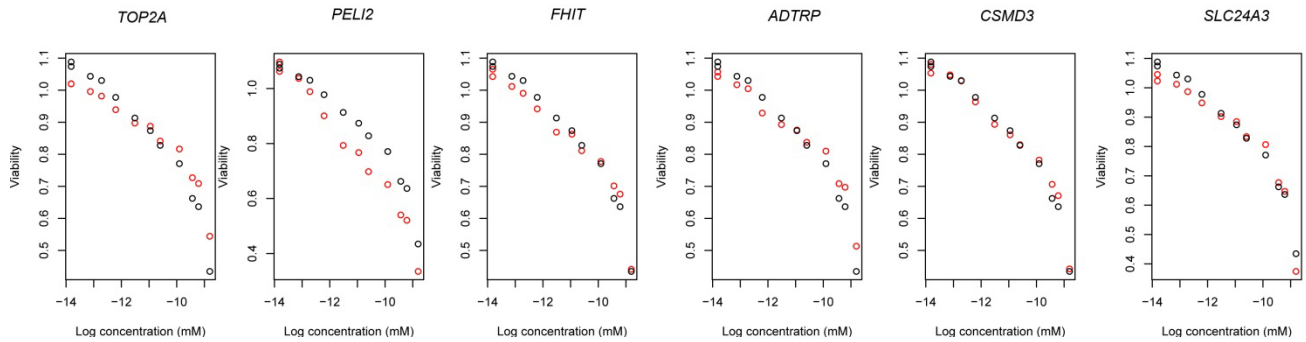
Supplemental Figure 1b:

CHORI line 032174

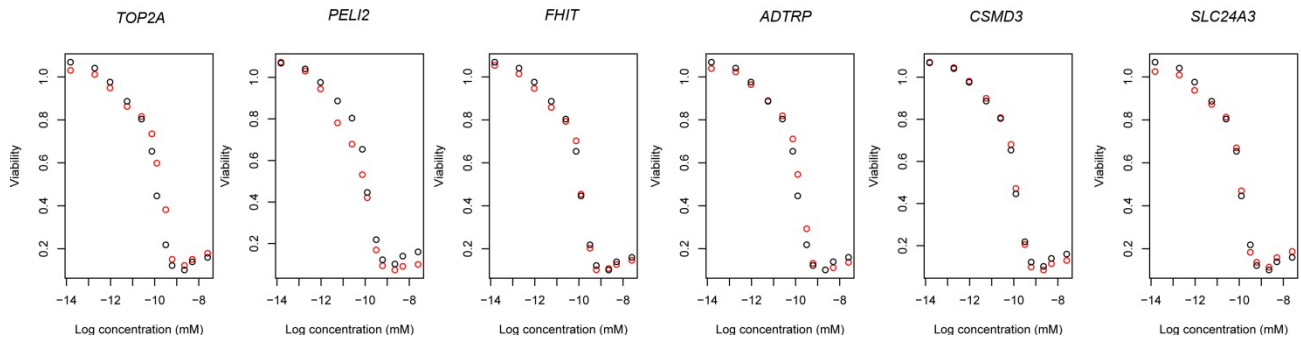
Daunorubicin response



Doxorubicin response



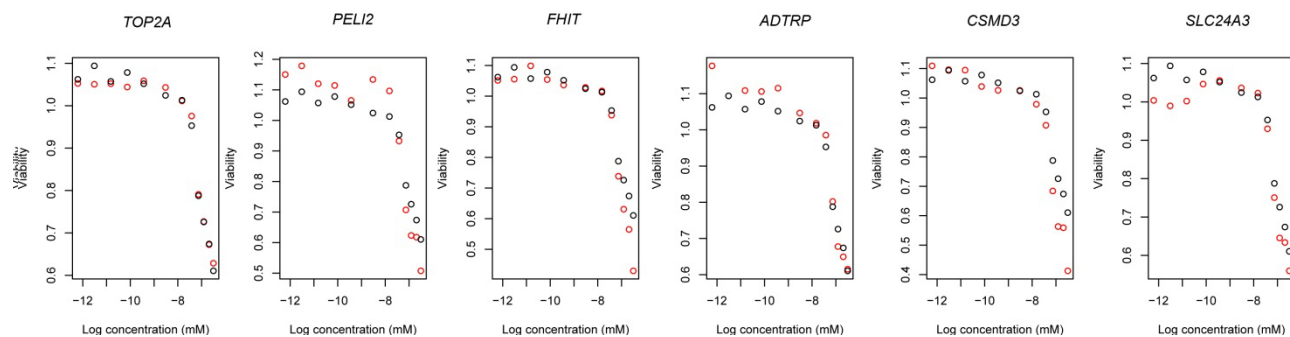
Epirubicin response



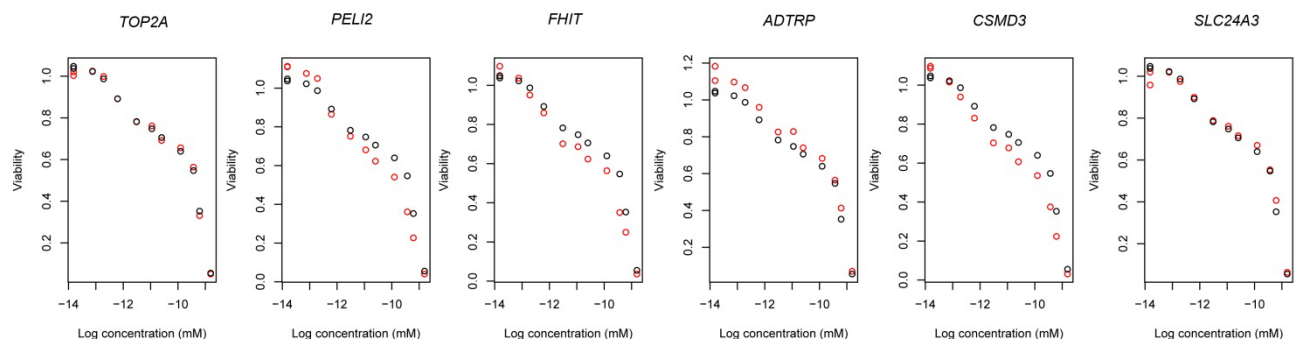
Supplemental Figure 1c:

CHORI line 040722

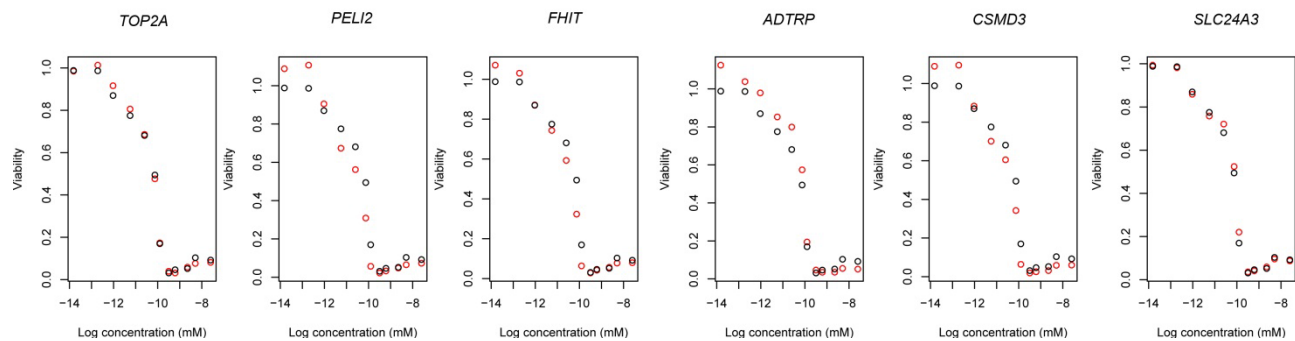
Daunorubicin response



Doxorubicin response



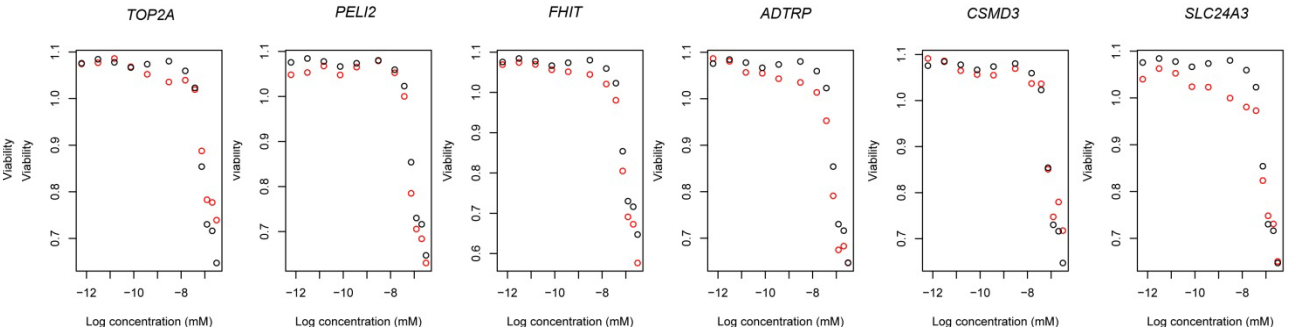
Epirubicin response



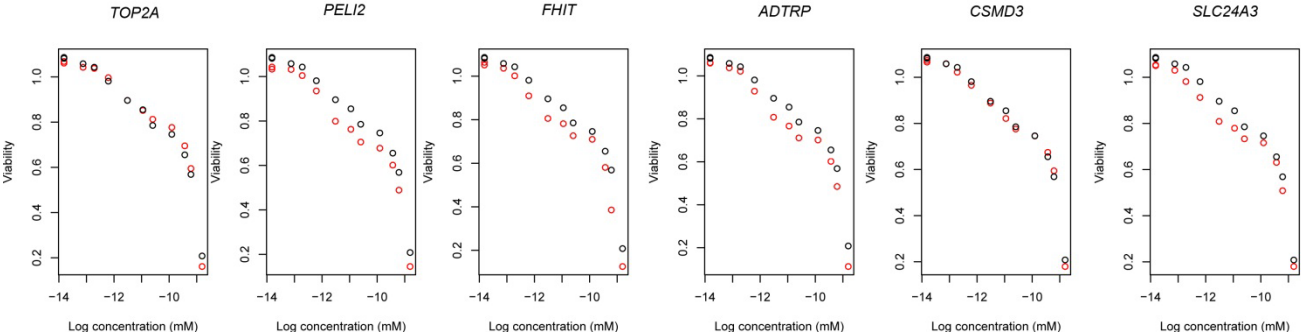
Supplemental Figure 1d:

CHORI line 031634

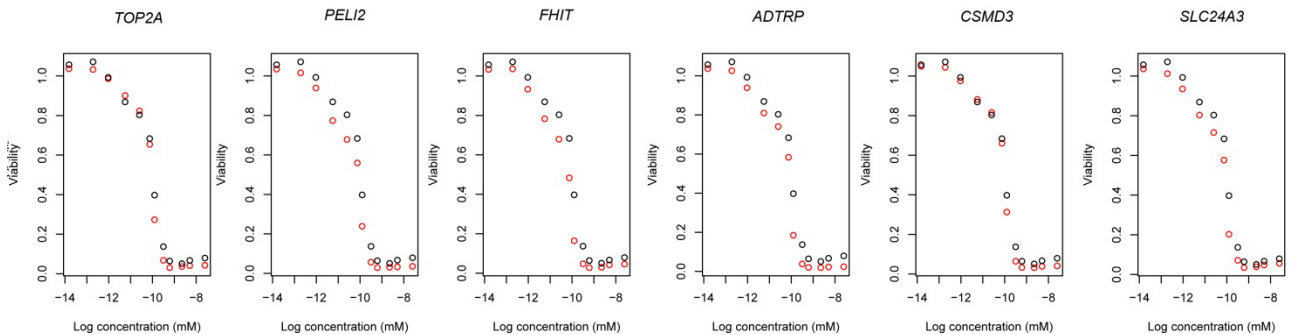
Daunorubicin response



Doxorubicin response



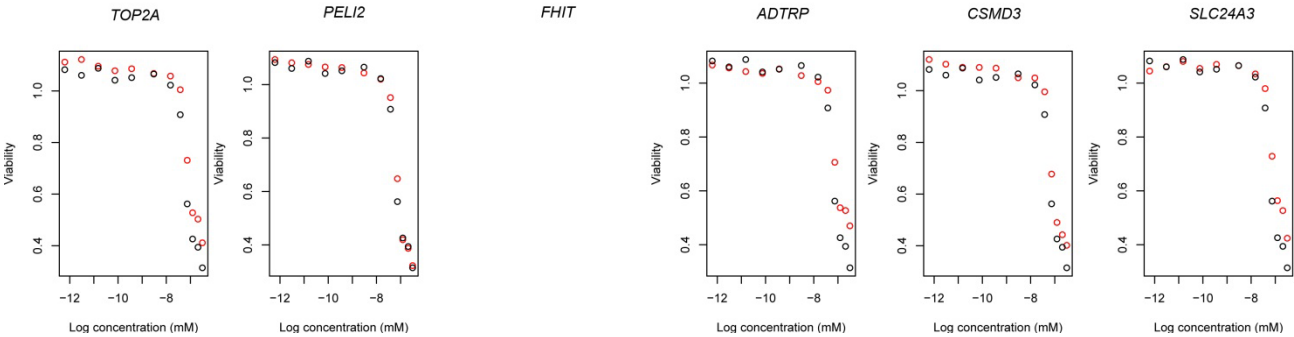
Epirubicin response



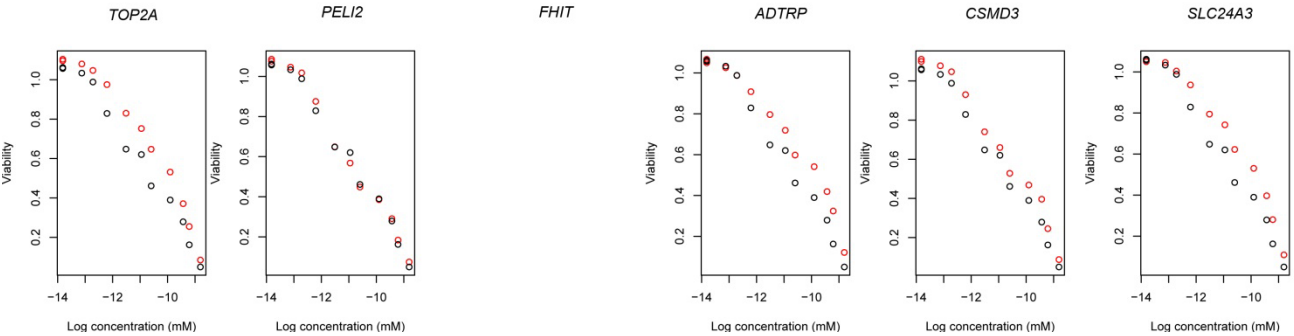
Supplemental Figure 1e:

CHORI line 030349

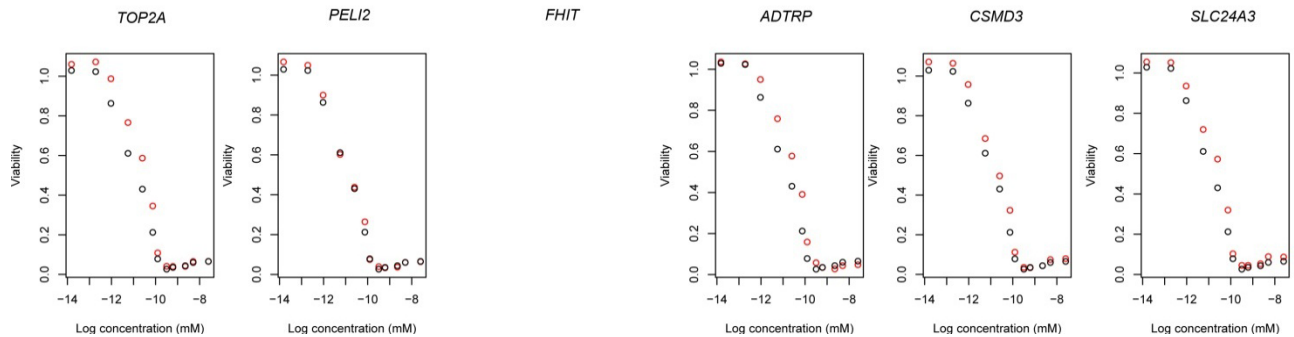
Daunorubicin response



Doxorubicin response



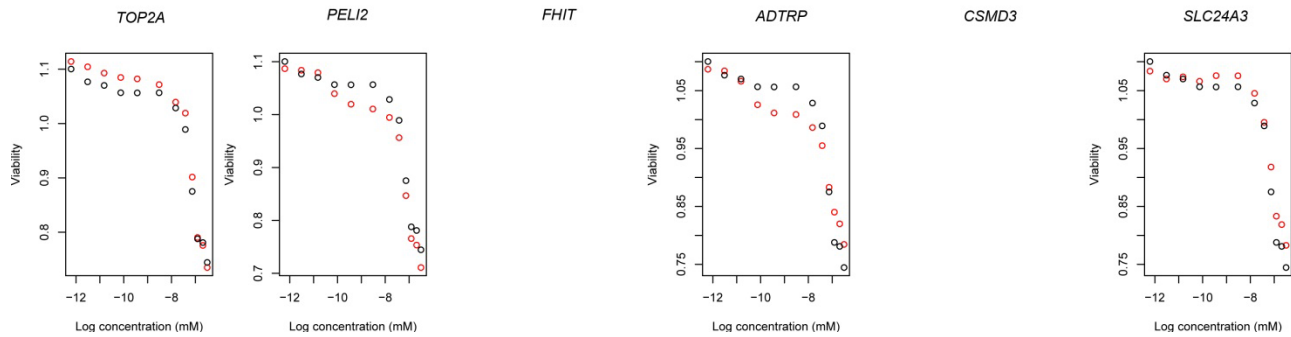
Epirubicin response



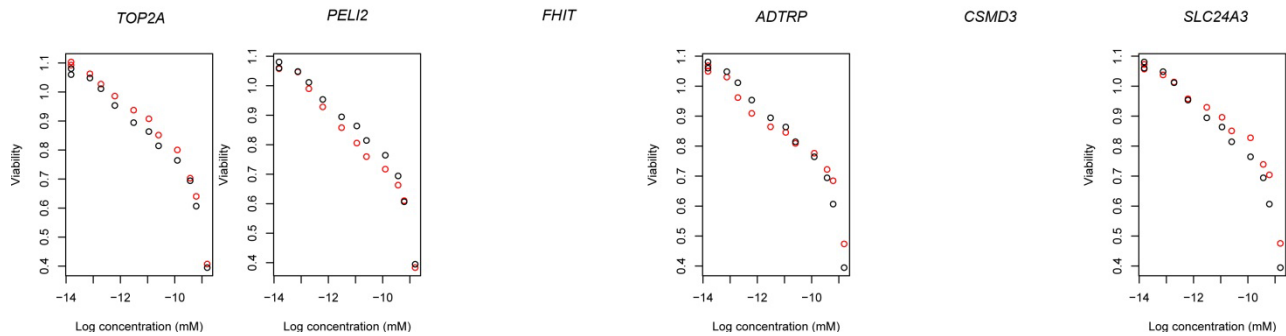
Supplemental Figure 1f:

CHORI line 021784

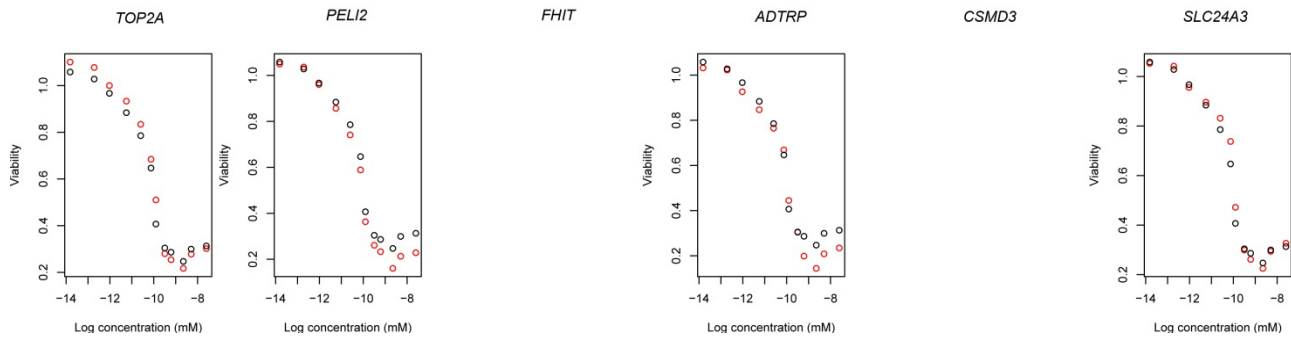
Daunorubicin response



Doxorubicin response



Epirubicin response



REFERENCES

1. Bates, S., *Progress towards personalized medicine*. Drug Discovery Today, 2010. **15**(3–4): p. 115-120.
2. Huang, S.-M., et al., *Application of Pharmacogenomics in Clinical Pharmacology*. Toxicology Mechanisms and Methods, 2006. **16**(2-3): p. 89-99.
3. Wheeler, H.E. and M.E. Dolan, *Lymphoblastoid cell lines in pharmacogenomic discovery and clinical translation*. Pharmacogenomics, 2011. **13**(1): p. 55-70.
4. Arcamone, F., *Adriamycin, 14-hydroxydaunomycin, a new antitumor antibiotic from S. peucetius var. caesius*. Biotechnology and bioengineering, 1969. **11**(6): p. 1101-10.
5. Cortés-Funes, H. and C. Coronado, *Role of anthracyclines in the era of targeted therapy*. Cardiovascular Toxicology, 2007. **7**(2): p. 56-60.
6. Weiss, R.B., *The anthracyclines: will we ever find a better doxorubicin?* Seminars in oncology, 1992. **19**(6): p. 670-86.
7. Kaye, S. and S. Merry, *Tumour cell resistance to anthracyclines — A review*. Cancer Chemotherapy and Pharmacology, 1985. **14**(2): p. 96-103.
8. Robert, J., *Pharmacokinetics and metabolism of anthracyclines*. Cancer surveys, 1993. **17**: p. 219-52.
9. Toffoli, G., et al., *Dose-finding and Pharmacologic Study of Chronic Oral Idarubicin Therapy in Metastatic Breast Cancer Patients*. Clinical Cancer Research, 2000. **6**(6): p. 2279-2287.
10. Thomas, X. and E. Archimbaud, *Mitoxantrone in the treatment of acute myelogenous leukemia: a review*. Hematology and Cell Therapy, 1997. **39**(4): p. 163-174.
11. Minotti, G., et al., *Anthracyclines: Molecular Advances and Pharmacologic Developments in Antitumor Activity and Cardiotoxicity*. Pharmacological Reviews, 2004. **56**(2): p. 185-229.
12. Gewirtz, D., *A critical evaluation of the mechanisms of action proposed for the antitumor effects of the anthracycline antibiotics adriamycin and daunorubicin*. Biochemical Pharmacology, 1999. **57**(7): p. 727-741.
13. Lal, S., et al., *Pharmacogenetics of Target Genes Across Doxorubicin Disposition Pathway: A Review*. Current Drug Metabolism, 2010. **11**(1): p. 115-128.
14. Momparler, R.L., et al., *Effect of Adriamycin on DNA, RNA, and Protein Synthesis in Cell-free Systems and Intact Cells*. Cancer Research, 1976. **36**(8): p. 2891-2895.

15. Ross, W.E., *Protein-associated DNA breaks in cells treated with adriamycin or ellipticine*. Biochimica et biophysica acta, 1978. **519**(1): p. 23-30.
16. Tewey, K.M., et al., *Adriamycin-Induced DNA Damage Mediated by Mammalian DNA Topoisomerase II*. Science, 1984. **226**(4673): p. 466-468.
17. Wassermann, K., *Effects of morpholinyl doxorubicins, doxorubicin, and actinomycin D on mammalian DNA topoisomerases I and II*. Molecular pharmacology, 1990. **38**(1): p. 38-45.
18. Perego, P., et al., *Role of Apoptosis and Apoptosis-Related Genes in Cellular Response and Antitumor Efficacy of Anthracyclines*. Current Medicinal Chemistry, 2001. **8**(1): p. 31-37.
19. Bertheau, P., et al., *Effect of mutated TP53 on response of advanced breast cancers to high-dose chemotherapy*. Lancet, 2002. **360**(9336): p. 852.
20. Szulawska, A., M. Gniazdowski, and M. Czyz, *Sequence specificity of formaldehyde-mediated covalent binding of anthracycline derivatives to DNA*. Biochemical Pharmacology, 2005. **69**(1): p. 7-17.
21. Cutts, S.M., et al., *Sequence Specificity of Adriamycin-DNA Adducts in Human Tumor Cells*. Molecular Cancer Therapeutics, 2003. **2**(7): p. 661-670.
22. Kiyomiya, K.-I., *The role of the proteasome in apoptosis induced by anthracycline anticancer agents*. International journal of oncology, 2002. **20**(6): p. 1205-9.
23. Torti, F.M., et al., *Reduced Cardiotoxicity of Doxorubicin Delivered on a Weekly Schedule*. Annals of Internal Medicine, 1983. **99**(6): p. 745.
24. Weijl, N.I., F.J. Cleton, and S. Osanto, *Free radicals and antioxidants in chemotherapy-induced toxicity*. Cancer Treatment Reviews, 1997. **23**(4): p. 209-240.
25. Wallace, K.B., *Adriamycin-induced interference with cardiac mitochondrial calcium homeostasis*. Cardiovascular Toxicology, 2007. **7**(2): p. 101-7.
26. Simůnek, T., *Anthracycline-induced cardiotoxicity: overview of studies examining the roles of oxidative stress and free cellular iron*. Pharmacological reports, 2009. **61**(1): p. 154-71.
27. Löwenberg, B., et al., *High-Dose Daunorubicin in Older Patients with Acute Myeloid Leukemia*. New England Journal of Medicine, 2009. **361**(13): p. 1235-1248.
28. Johnson_and_Johnson, *J&J Annual Report*, 2008, Johnson and Johnson.
29. Robert, J., *Epirubicin: Clinical Pharmacology and Dose-Effect Relationship*. Drugs, 1993. **45**: p. 20-30.

30. Eiermann, W., et al., *Dose-intensified epirubicin versus standard-dose epirubicin/cyclophosphamide followed by CMF in breast cancer patients with 10 or more positive lymph nodes: Results of a randomised trial (GABG-IV E-93) – The German Adjuvant Breast Cancer Group*. European journal of cancer (Oxford, England : 1990), 2010. **46**(1): p. 84-94.
31. Parsons, A.B., et al., *Exploring the Mode-of-Action of Bioactive Compounds by Chemical-Genetic Profiling in Yeast*. Cell, 2006. **126**(3): p. 611-625.
32. Whitehurst, A.W., et al., *Synthetic lethal screen identification of chemosensitizer loci in cancer cells*. Nature, 2007. **446**(7137): p. 815-819.
33. Watson, V.G., et al., *Identification and Replication of Loci Involved in Camptothecin-Induced Cytotoxicity Using CEPH Pedigrees*. PLoS ONE, 2011. **6**(5): p. e17561.
34. Auman, J.T. and H.L. McLeod, *Cancer Pharmacogenomics: DNA Genotyping and Gene Expression Profiling to Identify Molecular Determinants of Chemosensitivity*. Drug Metabolism Reviews, 2008. **40**(2): p. 303-315.
35. Simon, J.A., et al., *Phenotypic Predictors of Response to Simvastatin Therapy Among African-Americans and Caucasians: The Cholesterol and Pharmacogenetics (CAP) Study*. The American Journal of Cardiology, 2006. **97**(6): p. 843-850.
36. Peters, E.J., et al., *Pharmacogenomic characterization of US FDA-approved cytotoxic drugs*. Pharmacogenomics, 2011. **12**(10): p. 1407-1415.
37. Johnson, A.D., et al., *SNAP: a web-based tool for identification and annotation of proxy SNPs using HapMap*. Bioinformatics, 2008. **24**(24): p. 2938-2939.
38. Brown, C., et al., *A comparison of association methods for cytotoxicity mapping in pharmacogenomics*. Frontiers in Genetics, 2011. **2**.
39. Liu, P., et al., *Identification of Somatic Mutations in Non-Small Cell Lung Carcinomas Using Whole-Exome Sequencing*. Carcinogenesis, 2012.
40. Yu, K.-Y., et al., *Cutting Edge: Mouse Pellino-2 Modulates IL-1 and Lipopolysaccharide Signaling*. The Journal of Immunology, 2002. **169**(8): p. 4075-4078.
41. Schauvliege, R., S. Janssens, and R. Beyaert, *Pellino proteins are more than scaffold proteins in TLR/IL-1R signalling: A role as novel RING E3-ubiquitin-ligases*. FEBS Letters, 2006. **580**(19): p. 4697-4702.
42. Jensen, L.E. and A.S. Whitehead, *Pellino2 activates the mitogen activated protein kinase pathway*. FEBS Letters, 2003. **545**(2–3): p. 199-202.
43. Ai, L., et al., *Ataxia-Telangiectasia, mutated (ATM) / nuclear factor kappa light chain enhancer of activated B cells (NF kappaB) signaling controls basal and DNA damage-induced transglutaminase 2 expression*. Journal of Biological Chemistry, 2012.

44. Montagut, C., et al., *Activation of nuclear factor- κ B is linked to resistance to neoadjuvant chemotherapy in breast cancer patients*. *Endocrine-Related Cancer*, 2006. **13**(2): p. 607-616.
45. Bednarski, B.K., et al., *Active roles for inhibitory κ B kinases α and β in nuclear factor- κ B-mediated chemoresistance to doxorubicin*. *Molecular Cancer Therapeutics*, 2008. **7**(7): p. 1827-1835.
46. Bednarski, B.K., A.S. Baldwin, Jr., and H.J. Kim, *Addressing Reported Pro-Apoptotic Functions of NF- κ B: Targeted Inhibition of Canonical NF- κ B Enhances the Apoptotic Effects of Doxorubicin*. *PLoS ONE*, 2009. **4**(9): p. e6992.
47. Li, S., M. E, and B. Yu, *Adriamycin induces myocardium apoptosis through activation of nuclear factor κ B in rat*. *Molecular Biology Reports*, 2008. **35**(4): p. 489-494.
48. Bignold, L.P., *Embryonic reversions and lineage infidelities in tumour cells: genome-based models and role of genetic instability*. *International Journal of Experimental Pathology*, 2005. **86**(2): p. 67-79.
49. Pekarsky, Y., et al., *FHIT: from gene discovery to cancer treatment and prevention*. *The Lancet Oncology*, 2002. **3**(12): p. 748-754.
50. Hegi, M.E., et al., *MGMT Gene Silencing and Benefit from Temozolomide in Glioblastoma*. *New England Journal of Medicine*, 2005. **352**(10): p. 997-1003.